Nuclear Localization of KLF4 Is Associated with an Aggressive Phenotype in Early-Stage Breast Cancer

Ashka Y. Pandya,[1] Lynya I. Talley,[2] Andra R. Frost,[3] Thomas J. Fitzgerald,[2] Vivek Trivedi,[2] Mithun Chakravarthy,[3] David C. Chhieng,[3] William E. Grizzle,[3] Jeffrey A. Engler,[5] Helen Krontiras,[4] Kirby I. Bland,[4] Albert F. LoBuglio,[2] Susan M. Lobo-Ruppert,[2] and J. Michael Ruppert[2]

[1]Department of Cell Biology, [2]Department of Medicine, Division of Hematology/Oncology, [3]Department of Pathology, [4]Department of Surgery, and [5]Department of Biochemistry and Molecular Genetics, University of Alabama at Birmingham, Birmingham, Alabama

ABSTRACT

Purpose: **The Krüppel-like transcription factor KLF4/GKLF induces both malignant transformation and a slow-growth phenotype *in vitro*. Although KLF4 expression is increased in most cases of breast cancer, it was unknown whether these cases represent a distinct subtype with a different clinical outcome.**

Experimental Design: **We examined expression of KLF4 by immunostaining 146 cases of human primary infiltrating ductal carcinoma of the breast. Staining patterns were correlated with clinical outcome and with established prognostic factors.**

Results: **Subcellular localization exhibited case-to-case variation. Tumors with high nuclear staining and low cytoplasmic staining were termed type 1. For patients with early-stage disease (*i.e.*, stage I or IIA), type 1 staining was associated with eventual death because of breast cancer (hazard ratio, 2.8; 95% confidence interval, 1.23–6.58; $P = 0.011$). The association was stronger in patients with early-stage cancer and small primary tumors (*i.e.*, ≤2.0 cm in diameter; hazard ratio, 4.3; 95% confidence interval, 1.75–10.62; $P < 0.001$). For patients with early-stage disease, multivariate analysis indicated that type 1 staining was independently associated with outcome (adjusted hazard ratio 2.6; 95% confidence interval, 1.10–6.05; $P = 0.029$). Type 1 staining was also associated with high histological grade ($P = 0.032$), increased expression of Ki67 ($P = 0.016$), and reduced expression of BCL2 ($P = 0.032$). *In vitro*, KLF4 was localized within the nucleus of transformed RK3E epithelial cells, consistent with a nuclear function of this transcription factor during induction of malignant transformation.**

Conclusions: **The results suggest that localization of KLF4 in the nucleus of breast cancer cells is a prognostic factor and identify KLF4 as a marker of an aggressive phenotype in early-stage infiltrating ductal carcinoma.**

INTRODUCTION

Appropriate regulation of cellular proliferation and differentiation is important for embryonic development, tissue morphogenesis, and homeostasis and requires integration of diverse extracellular signals that program transcription and DNA replication within the nucleus. Within epithelial cells, pathways that transforming these signals are frequent targets of genetic alteration during progression to carcinoma (1, 2). A shared property of the transforming growth factor (TGF)-β, WNT, and Sonic Hedgehog pathways is the regulation of transcription factors by tethering within the cytoplasm. In normal tissues, these secreted morphogens signal through distinct receptors to induce translocation of latent transcription factors from the cytoplasm to the nucleus, resulting in activation of specific target genes such as *cyclin D1* and *c-MYC* (3, 4). Genetic alterations found in cancers can mimic signaling by a morphogen, resulting in inappropriate nuclear accumulation of oncogene-encoded transcription factors such as GLI, β-catenin, or γ-catenin/plakoglobin (5–10).

As with these transcription factors, a zinc finger protein of the Krüppel family termed KLF4 (or GKLF) exhibits potent transforming activity when expressed in cultured RK3E epithelial cells (11). A functional screen identified multiple independent cDNA clones of *KLF4* and *c-MYC*, implicating these molecules as major transforming activities in the human cancer cell lines examined. As shown by mRNA *in situ* hybridization analysis of tumor and adjacent normal tissue, *KLF4* expression is up-regulated in a majority of infiltrating ductal carcinomas of the breast and in virtually all squamous cell carcinomas of the oropharynx (11, 12). In contrast, expression in carcinomas of the prostate was unchanged or was down-regulated. Genetic studies in mice revealed that *Klf4* is dispensable for development *in utero* but critical for differentiation of skin and gut epithelium and for function of the skin as a water barrier in postnatal animals (13). Consistent with these results, in mouse and humans *KLF4* is normally expressed in nondividing, differentiated epithelial cells (11, 14, 15). The apparent deregulation of this potent transforming activity in tumors suggested that *KLF4* may contribute to tumor progression when inappropriately expressed in proliferation-competent cell types such as stem cells or transit amplifying cells within the epithelium (11, 12).

Received 10/28/03; revised 12/12/03; accepted 12/17/03.
Grant support: NIH Grants RO1 CA65686 (J. Ruppert), P50 CA89019 (K. Bland, J. Ruppert), T32 CA91078 (K. Bland), T32 DK07488 (T. Fitzgerald), and by a gift to the Comprehensive Cancer Center from the Avon Foundation.
The costs of publication of this article were defrayed in part by the payment of page charges. This article must therefore be hereby marked *advertisement* in accordance with 18 U.S.C. Section 1734 solely to indicate this fact.
Requests for reprints: J. Michael Ruppert, Department of Medicine, Room 570 WTI, University of Alabama at Birmingham School of Medicine, Birmingham, AL 35294-3300. Phone: (205) 975-0556; Fax: (205) 934-9511; E-mail: mruppert@uab.edu.

Another property of *KLF4* is the slow-growth phenotype induced in cultured cells, one of the early functional observations made for this zinc finger protein (15–18). Candidate mechanisms related to the slow-growth include transcriptional upregulation of *WAF1/CIP1* and repression of *CYCLIN D1* or ornithine decarboxylase. We observed the same slow-growth phenotype (11), as well as induction of *Waf1/Cip1*, in RK3E cells that were transformed by *KLF4*.[6] These malignant cells proliferate with a doubling time of 28 h, longer than for parental RK3E cells (12 h), for *c-MYC*- or *GLI*-transformed cells (18 h each), or for *RAS*-transformed cells (9 h). In summary, *KLF4* induces a complex phenotype that includes a reduced proliferation rate, induction of a spindled, mesenchymal-like cell morphology, loss-of-contact inhibition, and malignant transformation as indicated by tumorigenicity in mice (11).

KLF4 can function within the nucleus to regulate expression of specific target genes that contain promoter-proximal KLF4 response elements similar to the binding sequence 5′-$^{G}/_{A}$-$^{G}/_{A}$-G-G-$^{C}/_{T}$-G-$^{C}/_{T}$-3′ (19). However, few functional studies have demonstrated a requirement for nuclear localization because the nuclear localization signal is partially contained within the zinc fingers of the DNA binding domain (20–22). We previously used a mouse monoclonal antibody to human KLF4 (anti-KLF4) to analyze expression in multiple normal tissues and cancers (12). Specificity of the antibody was supported by analysis of the tissue sections by mRNA *in situ* hybridization and by virtue of cell-type and cancer-type specific patterns of expression *in vivo*. We observed that the subcellular localization is mixed, with prominent expression in both the nucleus and cytoplasm. More recently, similar results were obtained using a different anti-KLF4 antibody (23).

In the current study, we show that KLF4 exhibits distinct patterns of subcellular localization in different primary breast tumors. Preferential nuclear localization of KLF4 in surgically excised tumors of patients with early-stage disease correlated with eventual death because of breast cancer and with other parameters previously associated with increased risk of recurrence or death. Small primary tumors with preferential nuclear localization of KLF4 were much more likely to lead to death from breast cancer and may be distinct with respect to mechanisms of pathogenesis, mechanisms of metastasis, or response to specific therapies.

MATERIALS AND METHODS

Tissue Procurement and Study Patients. Archived paraffin blocks of formalin-fixed tissue corresponding to 146 cases of infiltrating ductal carcinoma of the breast, diagnosed between 1983 and 1995, were obtained from the Department of Pathology at the University of Alabama at Birmingham (Table 1). Approval for the study was obtained from the University of Alabama at Birmingham Institutional Review Board. Tumor size, axillary lymph node status, stage at diagnosis, treatment, and demographic information were obtained by review of pathology reports and clinical charts maintained in the Departments of Pathology and Surgery, respectively. All charts were independently reviewed by each of two coauthors (M. Chakravarthy, J. M. Ruppert), and discordances were reconciled. Follow-up information and cause of death was obtained from the University of Alabama at Birmingham Hospital Tumor Registry, which maintains an updated database through annual contact with primary care physicians. Stage at diagnosis was based upon tumor size (T), axillary lymph node status (N), and the presence of distant metastases (M) as described by the American Joint Committee on Cancer (Table 1; Ref. 24).

Table 1 Characteristics of the study population

	n	%
Demographics		
Age at diagnosis (yrs)		
≤50	68	47
>50	78	53
Race		
African American	42	29
Caucasian	104	71
Postoperative treatment (received treatment/total)		
Chemotherapy	70/142	49
Radiotherapy	41/142	29
Tamoxifen	72/133	54
Stage and tumor grade (high grade/total)		
Stage I	9/38	24
Stage IIA	32/59	54
Stage IIB	18/29	62
Stage III–IV	17/20	85
Outcome (death caused by breast cancer/total)		
Stage I	12/38	32
Stage IIA	11/59	19
Stage IIB	11/29	38
Stage III	9/15	60
Stage IV	4/5	80

Immunohistochemistry. Tissues were fixed in neutral-buffered formalin and embedded in paraffin. To avoid antigen decay, sections were cut to 5-μm thickness 1 day before immunostaining. Sections were attached to the slide by heating in a 60°C oven for 1 h. Deparaffinized tissue sections were treated for 5 min in a 3% aqueous solution of hydrogen peroxide, blocked in PBS with 3% goat serum (Sigma) for 1 h at room temperature, and then incubated for 1 h at room temperature with anti-KLF4 monoclonal antibody IE5 at 1.0 μg/ml in binding buffer (PBS containing 1% bovine serum albumin, 1 mM EDTA, and 0.01% sodium azide; Ref. 12). Anti-KLF4 was stored in aliquots at −85°C, and was stable through multiple freeze/thaw cycles. Activity is lost within weeks when stored at 4°C. Slides were washed in 50 mM Tris-HCl (pH 7.6), 150 mM NaCl, 0.01% (v/v) Triton X-100. Immunodetection was performed using a biotinylated secondary antibody, streptavidin-horseradish peroxidase (Signet Pathology Systems), and the chromogenic substrate diaminobenzidine (BioGenex). Sections were counterstained with Harris' hematoxylin (Surgipath). As controls, histological sections of each case were processed without the addition of primary antibody for each antigen retrieval method along with positive/negative, multi-tissue control sections.

For the detection of estrogen receptor (ER), progesterone receptor (PR), p27KIP1, and Ki67, histological sections were subjected to low temperature antigen retrieval with enzymatic pretreatment. This consisted of predigestion in 0.1% trypsin (type II-S from porcine pancreas; Sigma) in PBS for 15 min at

[6] Induction of *Waf1/Cip1* by KLF4 in RK3E cells is an unpublished observation by S. M. Lobo-Ruppert and J. M. Ruppert.

37°C, followed by incubation in 10 mM citrate buffer (pH 6) for 2 h at 80°C (25). The antibodies used were the anti-ER mouse monoclonal antibody, clone ER88 (0.33 mg/ml total protein; BioGenex) at 1:30 dilution, the anti-PR receptor mouse monoclonal antibody, clone PR88 (0.33 mg/ml total protein; BioGenex) at 1:30 dilution, anti-Ki67 mouse monoclonal antibody, clone MIB-1 (0.37 mg/ml total protein; BioGenex) at 1:30 dilution, and the anti-p27KIP1 mouse monoclonal antibody, clone 1B4 (8.0 μg/ml IgG; Novocastra Laboratories Ltd.) at 1:30 dilution. Immunostaining for BCL2 was preceded by incubation of histological sections in boiling 10 mM sodium citrate buffer (pH 6.0) for 10 min in a microwave oven (25). Anti-BCL2 (clone 124; Genosys Biotechnologies, Inc.) was used at 12.5 μg/ml. Anti-ERBB2 (clone 3B5; Oncogene Research Products) was used at 0.25 μg/ml. Anti-p53 (clone BP53.12; Oncogene Research Products) was used at 0.25 μg/ml.

Immunoscoring. The intensity of immunostaining of individual cells was scored on a scale of 0 (no staining) to 4 (strongest intensity), and the percentage of cells with staining at each intensity was estimated. For ERBB2, only membranous staining was assessed. The proportion of cells at each intensity was multiplied by the corresponding intensity value, and these products were added to obtain an immunostaining score (immunoscore) ranging from 0 to 4 (26, 27). All slides were examined and scored independently by two investigators (A. R. Frost, D. C. Chhieng, or J. M. Ruppert), large discordances were reconciled by reexamination of the slide, and the scores were then averaged.

Histological Grading. The Nottingham modification of the Bloom and Richardson histological grading system was used to categorize carcinomas as high grade, corresponding to a total score of 8 or 9, or low-to-moderate grade (referred to as low), corresponding to a total score of <8 (28).

Statistical Analysis. Median immunoscores were used to group cases with high or low expression levels of KLF4, Ki67, BCL2, ERBB2, or P27KIP1. For ER, PR, and p53, tumors with $>10\%$ positive cells were scored as positive. Associations of clinical, pathological, and demographic factors with KLF4 staining patterns were evaluated using the Mantel-Haenszel χ^2 test or, where appropriate, Fisher's exact test (29). Kaplan-Meier methods were used to compare overall survival rates and significance was assessed using the log-rank test (30). Survival time was defined as the interval from the date of diagnosis to the date of death. Patients who were alive at the last date of contact, died from unknown causes or died from causes other than breast cancer were censored at the date of last contact.

Multivariate Cox proportional hazards models were performed to evaluate the effect of KLF4 staining patterns on survival while controlling for the effects of extraneous factors (31). The analysis was performed using a stepwise selection technique. Included in the full model were KLF4, race, chemotherapy, stage, histological grade, ER, and PR. Significance level to stay in the model was set at 0.050. In addition, interaction terms were included in the model to evaluate the multiplicative effect of KLF4 staining patterns and various clinical or pathological factors on survival. All significance tests were two-sided with $\alpha = 0.05$.

Plasmid Construction and Analysis of *in Vitro* Transforming Activity. The human KLF4 cDNA was modified at the NH_2 terminus with the hemagglutinin (HA) epitope (32) and cloned into the Moloney murine leukemia virus vector pLJD (obtained from L. T. Chow, University of Alabama at Birmingham). Cell culture, retroviral transduction of RK3E cells (33), and assay of transforming activity were performed as described previously (11). For focus assays, transduced cells were maintained for 4 weeks in nonselective growth media. For colony morphology assays, transduced cells were selected in 400 μg/ml G418, and colony morphology was scored 4 weeks later. A population derived from >1000 independently transduced cells was passaged in selective medium and then assayed for expression of HA-KLF4 by immunofluorescence.

Subcellular Localization of Epitope-Tagged KLF4. The HA-KLF4 cDNA was inserted into pRK5 adjacent to the cytomegalovirus immediate early promoter-enhancer. HEK293 embryonic kidney epithelial cells were plated on poly-L-lysine coated coverslips, grown to 50% confluence, then transfected using the lipid reagent transIT-LT1 (Mirus). To enable identification of transfected cells, a green fluorescent protein expression vector (pEGFP; Clontech) was included in the transfection mixture. Cells were fixed in 4% paraformaldehyde in PBS for 10 min at room temperature, treated with 0.5% Triton X-100 in PBS for 10 min at 4°C, and then blocked in 50% (v/v) goat serum in PBS (blocking solution). Anti-HA monoclonal antibody 12CA5 (Roche) was used at 4.0 μg/ml in blocking solution for 45 min in a humidified chamber. Bound antibody was detected using goat antimouse IgG conjugated to Alexa Fluor 594 (Molecular Probes). Where indicated, the cytoplasm was stained using Alexa Fluor 488 phalloidin (Molecular Probes). Nuclei were stained using 4′,6-diamidino-2-phenylindole at 0.3 μM in PBS, rinsed briefly, mounted using Prolong Antifade medium (Molecular Probes), and then stored in the dark at −20°C for subsequent examination.

RK3E epithelial cells stably transduced with pLJD-HA-KLF4 (see above) were analyzed for expression of the transgene in similar fashion. Fluorescence of the secondary antibody, cotransfected green fluorescent protein, phalloidin, or 4′,6-diamidino-2-phenylindole were visualized using an Axioplan 2 Imaging microscope equipped with an external filter wheel (Zeiss). Black and white images were collected using an AxioCam HRc digital camera, and the pseudo-colored images were merged using Axiovision software (version 3.1).

RESULTS

Characteristics of the Patients. We previously reported that expression of KLF4 is up-regulated in most cases of infiltrating ductal carcinoma of the breast (12). To determine whether expression of KLF4 is associated with other properties of breast tumors, we identified 146 cases of infiltrating ductal carcinoma that were well characterized for clinical and pathological parameters, including surgical management, stage at diagnosis, histological grade, postoperative therapy, and cause of death (Table 1). A total of 134 of the 146 patients (92%) underwent axillary lymph node dissection with at least five lymph nodes sampled, and ≥ 10 lymph nodes were sampled for 116 patients (79%). The median follow-up from the time of diagnosis was 7.1 years. Patients with early-stage disease (*i.e.*, stages I and IIA) exhibited a 5-year disease specific survival rate of 87% (*e.g.*, see below, Fig. 2*B*), similar to that observed in larger studies (34, 35). Likewise, patients with stage IIB, stage

III, or stage IV disease exhibited 5-year survival rates (75, 37, or 20%, respectively) similar to rates observed for larger groups. We analyzed expression of KLF4 and other prognostic or predictive factors, including the steroid hormone receptors ER and PR, the receptor tyrosine kinase ERBB2, the proliferation marker Ki67, the tumor suppressor p53, and two markers associated with favorable clinical outcome, BCL2 and the cyclin-dependent kinase inhibitor p27KIP1 (36).

Distinct Patterns of KLF4 Subcellular Localization in Breast Tumors. Overall, expression was detected in >90% of cases. Primary tumors varied greatly in their relative staining of the nucleus and cytoplasm (Fig. 1*A*). The pattern of subcellular localization within individual tumors was quite uniform across a histological section, and was similar in invasive and *in situ* components within the same section (Fig. 1*A* and data not shown). Scatterplot analysis demonstrated the spectrum of staining patterns observed in these tumors (Fig. 1*B*). On the basis of the four quadrants defined by the median immunostaining scores, tumors were classified as type 1, 2, 3, or 4. Type 1 tumors exhibit higher than median nuclear staining and lower than median cytoplasmic staining. Type 2 tumors have lower staining in each compartment. Type 3 tumors have predominantly cytoplasmic staining, and Type 4 tumors have increased staining in each compartment.

As KLF4 is likely to function in the nucleus rather than in the cytoplasm, we evaluated the impact of preferential nuclear expression of KLF4 on survival (Fig. 2*A*). We compared type 1

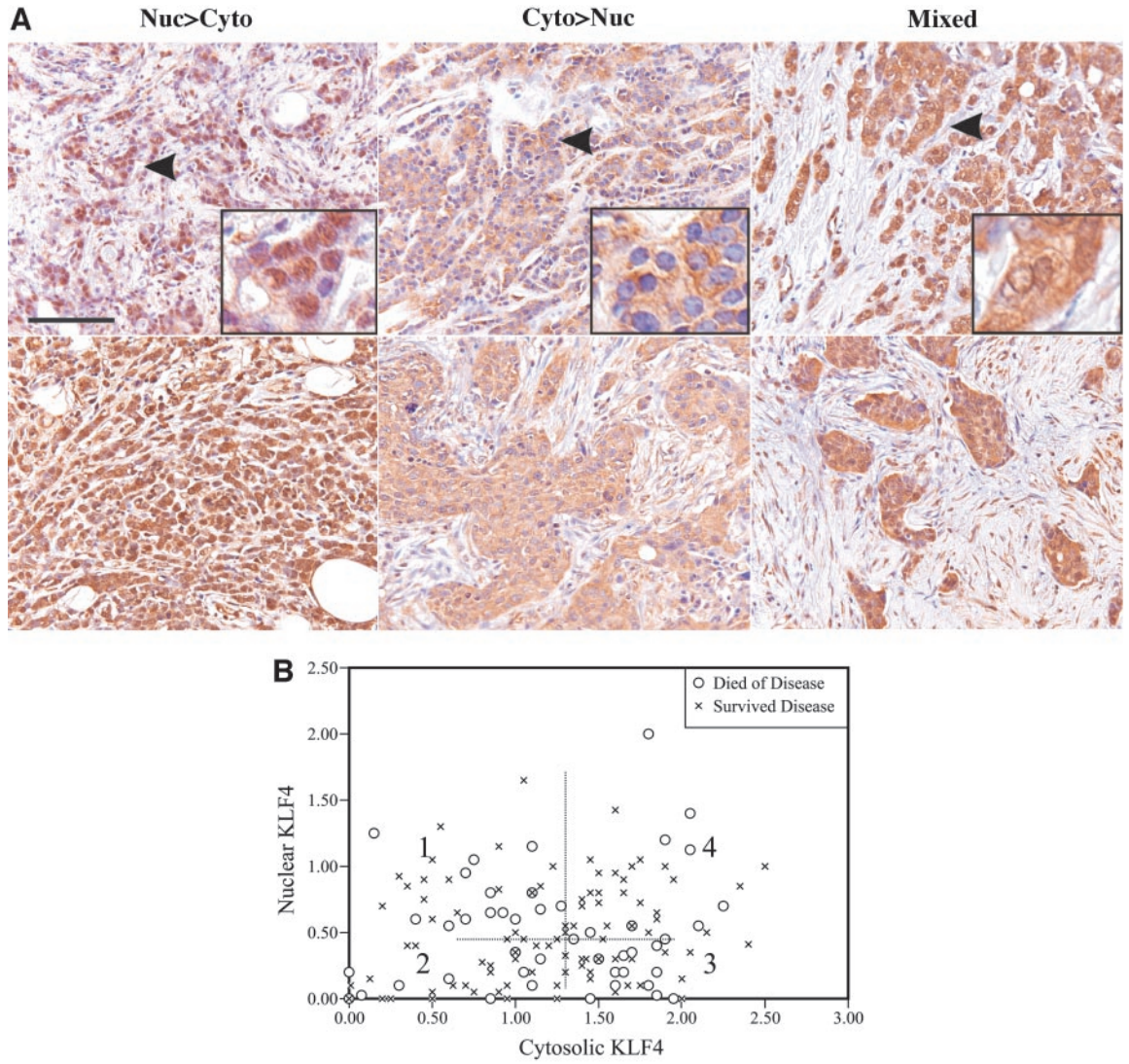

Fig. 1 Immunostaining of human breast cancers with anti-KLF4 monoclonal antibody. *A*, each panel illustrates a different case of primary breast cancer. Staining patterns were predominantly nuclear (*left panels*), predominantly cytoplasmic (*middle panels*), or mixed nuclear and cytoplasmic (*right panels*). Staining is indicated as a *brown* precipitate. Unstained nuclei appear *blue* because of the hematoxylin counterstain. *Arrowheads* indicate the area detailed at higher-fold magnification in the *inset*. *B*, scatterplot analysis of 146 cases of primary-infiltrating ductal carcinoma of the breast. Nuclear and cytosolic staining was scored on a scale from 0 to 4.0, where 0 represents no detectable staining and 4.0 represents saturation. A *broken line* indicates the median score for nuclear (0.45) or cytoplasmic (1.29) staining. Some data points represent two or more cases with the same score. The quadrants defined by the median scores were used to designate the KLF4 staining pattern as types 1, 2, 3, or 4. *Scale bar* for $A = 100$ μm.

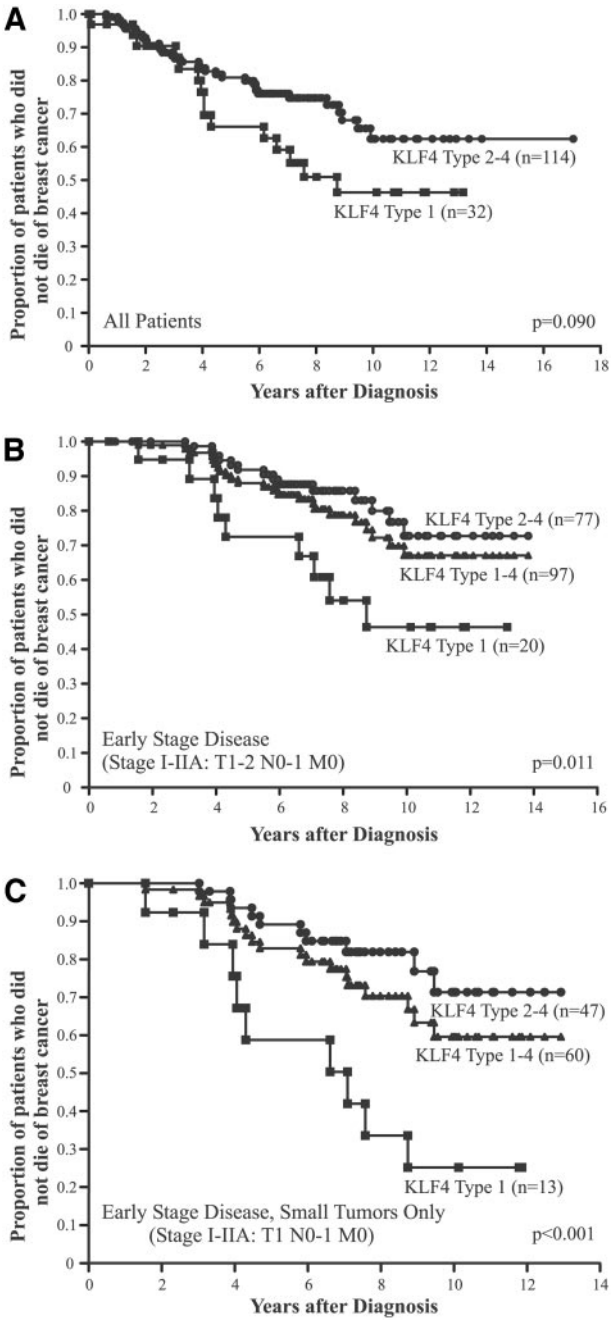

Fig. 2 Kaplan-Meier estimate of disease-specific survival according to KLF4 staining pattern. *A*, all patients regardless of stage at diagnosis. *B*, patients with early-stage disease only. *C*, patients with early-stage disease and small primary tumors. *n*, the number of patients in each group. Type 1 indicates tumors with nuclear staining >median and cytosolic staining <median, and type 2–4 indicates all other cases.

tumors to all other tumors combined (referred to as type 2–4). Although type 1 tumors appeared to be more often associated with death from breast cancer, this trend was not statistically significant (log-rank test, $P = 0.090$). No significant differences were obtained by comparison of type 3 tumors *versus* all others ($P = 0.227$). Likewise, tumors with high *versus* low nuclear expression exhibited similar outcomes (*i.e.*, using the median score as cutoff; $P = 0.601$), as did tumors with high *versus* low cytoplasmic expression ($P = 0.157$).

KLF4 Expression in Small Primary Tumors. The trend observed for all cases combined was more pronounced for patients who were diagnosed with early-stage cancer (*i.e.*, stages I and IIA; Fig. 2*B*; $P = 0.011$). Tabulation of outcome by stage and KLF4 staining pattern suggested an important role for size of the primary tumor in the association of KLF4 with clinical outcome (Table 2). Indeed, all 9 of the deaths among patients with type 1 staining and early-stage disease occurred in the setting of a small primary tumor (*i.e.*, ≤2.0 cm in diameter, indicated as T1). For the 7 patients with $T_1N_0M_0$ (*i.e.*, stage I) disease and type 1 staining, all but 2 succumbed to breast cancer. In contrast, none of the 7 patients who had $T_2N_0M_0$ (stage IIA) disease with type 1 staining died from breast cancer ($P = 0.010$). The median follow-up time for these groups was 4.30 years (stage I) and 8.01 years (stage IIA). Thus, patients with early-stage disease and small primary tumors were much more likely to die from breast cancer when the KLF4 staining pattern was type 1 (Fig. 2*C*; $P < 0.001$).

We used scatterplot analysis to examine the role of tumor size in the association of type 1 staining and death due to breast cancer (Fig. 3*A*). For patients with type 1 tumors that were ≤2.0 cm, 11 of 15 (73%) died from breast cancer. For patients with type 1 tumors in the range of 2.01–3.00 cm in size, only 2 of 9 (22%) died from breast cancer ($P = 0.033$). Thus, type 1 staining identifies a paradoxical subset of cancers in which larger tumor size is associated with a lower rate of death from breast cancer. No such effect was observed for patients with type 2–4 staining (Fig. 3*B*). This analysis suggests that any increased risk associated with type 1 staining may be limited to tumors ≤2.0 cm in diameter.

Despite the specific association between type 1 staining and outcome in small tumors, there was no difference in the overall staining pattern in small *versus* large tumors (Figs. 4, *A* and *B*). As with the distribution of scores in the two-dimensional plot (Fig. 4, *A* and *B*, *left panels*), the median immunoscores for each subcellular compartment were very similar (for small tumors: cytoplasm = 1.30, nucleus = 0.43; for large tumors, cytoplasm = 1.25, nucleus = 0.45). Survival analysis of all patients in the study, regardless of stage at diagnosis, demonstrated the specific association of type 1 staining and outcome in small tumors (Fig. 4*A*, *right panel*; $P < 0.001$). For large tumors, there was no trend toward a worse outcome in patients with type 1 staining (Fig. 4*B*, *right panel*; $P = 0.398$). As a control for the quality of the outcome data for each of the two subgroups, Kaplan-Meier analysis revealed that high histological grade was associated with death caused by breast cancer in both the small tumor ($P = 0.002$) and large tumor subgroups ($P = 0.026$; data not shown).

Association of the Type 1 Staining Pattern with Other Parameters. These results suggest that T1-type 1 tumors are more likely to recur as distant metastatic lesions, often several years later, leading to eventual death from breast cancer. To better characterize this potentially important subset of tumors, we determined whether other known prognostic factors are associated with type 1 staining (Table 3). Associations were tested for small tumors alone, for large tumors alone, and for all

Table 2 Proportion of patients surviving breast cancer through the follow-up period by stage at diagnosis and KLF4 staining pattern

Stage of disease at diagnosis	KLF4 staining pattern		
	Type 1 (n = 32) Survived/total (%)	Type 2–4 (n = 114) Survived/total (%)	P^a
Stage I ($T_1N_0M_0$)	2/7 (28)	24/31 (77)	**0.022**
Stage IIA ($T_1N_1M_0$)	2/6 (33)	13/16 (81)	**0.054**
Stage IIA ($T_2N_0M_0$)	7/7 (100)	26/30 (87)	0.570
Stage IIB ($T_2N_1M_0$, $T_3N_0M_0$)	5/7 (71)	13/22 (59)	0.676
Stage III–IV (T_1 only)	0/2 (0)	1/2 (50)	0.500
Stage III–IV (T_2–T_4)	1/3 (33)	5/13 (38)	1.00

[a] Values <0.100, representing trends or significant differences, are shown in bold.

tumors combined. Compared with patients with T1-type 2–4 lesions, patients with T1-type 1 lesions did not exhibit a significant difference in stage at diagnosis (P = 0.171). However, high histological grade was associated with type 1 staining in small tumors. A high grade was observed in 9 of 15 T1-type 1 cancers (60%). In contrast, only 14 of 49 (29%) T1-type 2–4 tumors exhibited high grade (P = 0.026). For large tumors, no association of histological grade with type 1 staining was observed (P = 0.252). For small and large tumors combined, histological grade was more often high in type 1 than in type 2–4 tumors (P = 0.032).

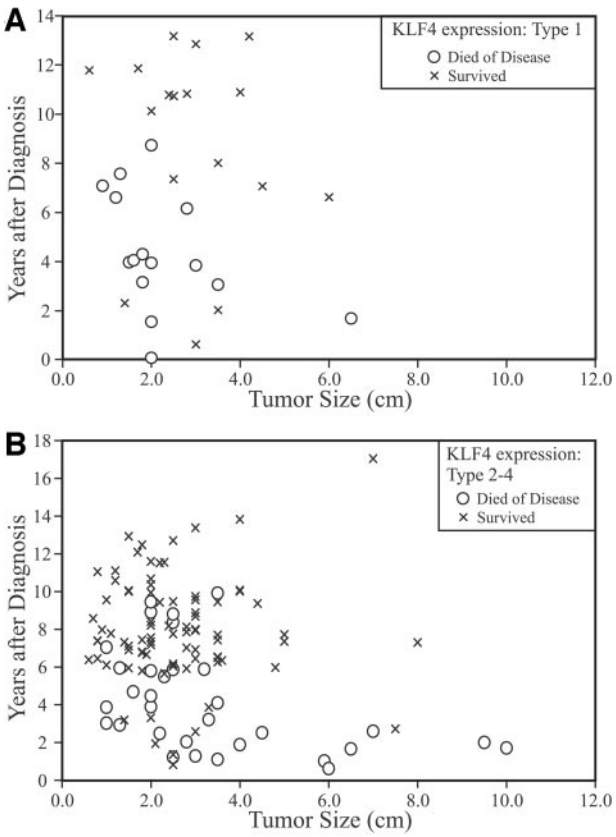

Fig. 3 Scatterplot analysis of disease-specific survival (years after diagnosis) according to tumor size and KLF4 staining pattern. *A*, patients with type 1 staining. *B*, all other patients (*i.e.*, type 2–4 staining).

Two immunohistochemical markers exhibited significantly different expression in type 1 *versus* type 2–4 tumors (all tumors combined). Expression of the proliferation marker Ki67 was more often high for tumors with type 1 staining patterns (P = 0.016). BCL2, for which higher expression was previously associated with a more favorable prognosis (37), was often low in type 1 tumors (P = 0.032). The observed associations additionally define the properties of T1-type 1 tumors. In summary, this group of clinically aggressive tumors is more likely to exhibit high histological grade, increased proliferation, and reduced expression of the favorable prognostic marker BCL2.

Univariate and Multivariate Analysis. We determined the unadjusted hazard ratio associated with type 1 staining for three groups of patients: all patients regardless of stage at diagnosis; patients with early-stage disease at diagnosis; and patients diagnosed with small primary tumors in the setting of early-stage disease (Table 4). Statistical significance was indicated when the 95% confidence interval (CI) of the hazard ratio excluded 1.00. For all patients (n = 146), factors significantly associated with a poorer survival included higher stage at diagnosis (hazard ratio, 5.5; 95% CI, 2.88–10.64), positive axillary lymph node status (hazard ratio 3.2; 95% CI, 1.65–6.22), high histological grade (hazard ratio, 2.8; 95% CI, 1.53–5.24), African-American race (hazard ratio, 2.3; 95% CI, 1.29–4.12), and reduced expression of BCL2 (hazard ratio, 0.4; 95% CI, 0.23–0.83). For patients with early stage cancer (n = 97), only type 1 staining exhibited a significant association with poor outcome (hazard ratio, 2.8; 95% CI, 1.23–6.58). For small tumors in the setting of early-stage cancer (n = 60), type 1 staining (hazard ratio, 4.3; 95% CI, 1.75–10.62), high histological grade (hazard ratio, 3.3; 95% CI, 1.32–8.28), and African-American race (hazard ratio, 2.6; 95% CI, 1.03–6.45) were each significant. In this smaller group of patients, other parameters previously associated with outcome in breast cancer exhibited the expected trend but did not reach statistical significance (*e.g.*, axillary lymph node status, stage, age, BCL2, P27KIP1, ER, and PR).

Multivariate analysis indicated that type 1 staining is independently associated with outcome in patients with early-stage disease. For all patients with stage I or stage IIA disease, KLF4 was the only significant variable remaining, with an adjusted hazard ratio of 2.6 (95% CI, 1.10–6.05; P = 0.029). The failure of other known risk factors such as nodal status, stage, or ER status to exhibit significance is attributed to the small sample

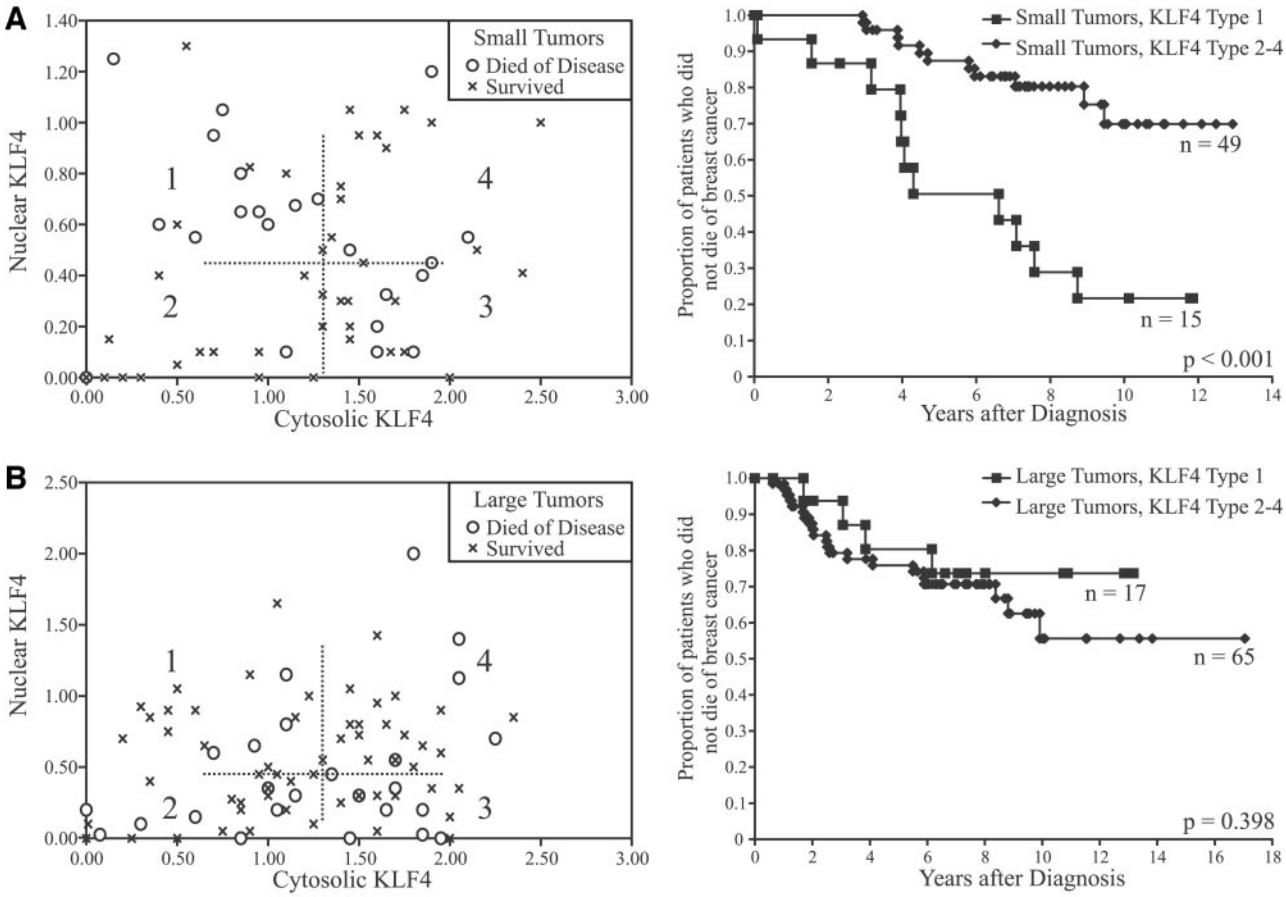

Fig. 4 Disease-specific survival according to KLF4 staining pattern in small and large breast tumors (all stages of disease). *A*, small tumors (≤2.0 cm in diameter in greatest dimension). *B*, large tumors (>2.0 cm in greatest dimension). Scatterplot (*left panels*) and Kaplan-Meier analysis (*right panels*) are shown. *Broken lines* (*left panels*) indicate the median scores in the cytosol and nucleus for all patients combined. For the scatterplots, some scores were adjusted by +/− 0.05 so that each case in the study is represented by a distinct data point.

size of this initial study and to the exclusion of patients with later stage disease from the model.

Analysis of KLF4 Subcellular Localization *in Vitro*. These results indicate that subcellular localization of KLF4 exhibits case-to-case differences in breast cancer and that preferential nuclear localization may be associated with an adverse outcome. Whether KLF4 functions within the nucleus or cytoplasm to induce transformation *in vitro* is unknown. We therefore asked whether KLF4 exhibits localization to the nucleus in transformed RK3E cells *in vitro* as observed in the more aggressive subset of early-stage breast cancer (T1-type 1 tumors).

We added a HA epitope to the NH_2 terminus of human wild-type KLF4 and confirmed the sequence of the final expression construct. To determine whether HA-KLF4 retains similar transforming activity as wild-type, we generated retroviral supernatants as described previously (11). Within 3 weeks after transduction of RK3E epithelial cells, wild-type KLF4 and HA-KLF4 each induced numerous transformed foci upon a background monolayer of contact-inhibited RK3E cells (data not shown). Cells transduced by the empty vector served as a negative control. As an additional measure of transforming activity, we used the colony morphology assay (11). We examined the morphology of cells within established colonies of RK3E cells that survived retroviral transduction and culture in selective growth medium. Unlike the vector control cells, HA-KLF4 cells and KLF4 cells were spindled, highly refractile, and formed dense colonies. These results indicate that HA-KLF4 retains the transforming activity of wild-type human KLF4.

To test whether the epitope enables identification of HA-KLF4, we first examined human embryonic kidney cells, termed HEK293, 48 h after transfection of the expression vector pRK5-HA-KLF4 or a vector control (Fig. 5*A*). HA-KLF4 exhibited two frequent patterns of subcellular localization. In a subset of cells, expression was localized almost entirely within the nucleus. In another subset, representing approximately one-half of all positive cells, nuclear staining was associated with a prominent rim of perinuclear staining (Fig. 5*A*, *middle panel*, *inset*). KLF4 expression in the cytoplasm was rarely observed to extend throughout the full extent of the cytoplasm, as shown by coexpression of a green fluorescent protein control (Fig. 5*A*, *right panel*). Similar results were obtained by transfection of MCF7 cells, although the perinuclear rim in these cells was somewhat thinner (data not shown). These results provide evidence for a cytosolic anchoring mechanism that may localize KLF4 to the perinuclear region in cultured

Table 3 Association of clinical, pathological, or immunohistochemical parameters with KLF4 staining patterns in breast tumors

Parameter	Small tumors only (T ≤ 2.0 cm)			Large tumors only (T > 2.0 cm)		
	KLF4 Type 1 (n = 15)	KLF4 Type 2–4 (n = 49)	P	KLF4 Type 1 (n = 17)	KLF4 Type 2–4 (n = 65)	P
Stage of disease at diagnosis						
Stage I	7/15 (47%)	31/49 (63%)		N/A	N/A	N/A
Stage IIA	6/15 (40%)	16/49 (33%)	0.171	7/17 (41%)	30/65 (46%)	0.714
Stage >IIA	2/15 (13%)	2/49 (4%)		10/17 (59%)	35/65 (54%)	
Histological grade						
High grade	9/15 (60%)	14/49 (29%)	**0.026**	13/17 (76%)	40/65 (62%)	0.252
Marker expression						
Ki67 high	9/15 (60%)	10/31 (32%)	**0.076**	14/16 (88%)	27/45 (60%)	**0.044**
BCL2 high	6/15 (40%)	21/31 (68%)	**0.073**	4/16 (25%)	21/45 (47%)	0.133
ERBB2 high	5/15 (33%)	17/31 (55%)	0.171	8/16 (50%)	22/45 (49%)	0.939
p53 positive	4/14 (29%)	3/30 (10%)	0.184	3/16 (19%)	15/50 (30%)	0.524
Estrogen receptor positive	11/15 (73%)	30/40 (75%)	1.00	6/17 (35%)	29/62 (47%)	0.428
Progesterone receptor positive	9/15 (60%)	22/41 (54%)	0.673	4/17 (24%)	21/61 (34%)	0.400
P27KIP1 high	6/15 (40%)	18/31 (58%)	0.250	8/16 (50%)	19/45 (42%)	0.591

[a] P refer to the behavior of the parameter in tumors with predominately nuclear expression of KLF4 (type 1; Fig. 1*B*) versus tumors with other expression patterns (type 2–4). Values < 0.100, representing trends or significant differences, are shown in bold. For small and large tumors combined, significant differences were observed for histological grade (P = 0.032), Ki67 (P = 0.016), and BCL2 (P = 0.032).

epithelial cells, analogous to mechanisms that regulate other transcription factor oncogenes.

To determine where KLF4 is located within transformed RK3E cells, stably transduced HA-KLF4 cells and vector control cells were passaged in culture, stained with anti-HA, and then examined by microscopy (Fig. 5*B*). Similarly as for HEK293 cells, the vast majority of expression was localized to the nucleus of transformed RK3E cells. In these cells, perinuclear or cytoplasmic staining was rarely detected (*i.e.*, in <5 of 100 cells examined). These results are consistent with a nuclear function of KLF4 during induction of malignant transformation *in vitro*.

DISCUSSION

Expression of KLF4 mRNA and protein was previously analyzed by immunostaining and by mRNA *in situ* hybridization analysis of breast cancers (12). As compared with adjacent, uninvolved epithelium, expression of this potent transforming activity is increased in the vast majority of breast tumors. In contrast, other tumor types such as colorectal or prostatic carcinoma do not exhibit increased expression (12). In the current study, we examined an additional 146 cases of breast cancer to determine whether expression of KLF4 is associated with specific clinical, pathological, or molecular features. Although overall expression of KLF4 was not associated with clinical outcome, we found that breast tumors exhibit marked case-to-case variation in subcellular localization. Preferential nuclear localization (*i.e.*, type 1 staining) was associated with clinical outcome in early-stage cancer, and this association was only apparent when the primary tumor size was small (*i.e.*, ≤2 cm in diameter, designated as T1).

Although type 1 staining was strongly associated with a poor

Table 4 Cox regression analysis (unadjusted hazard ratios and 95% confidence intervals): associations with disease-specific survival[a]

	All tumors[b]		Stage I and IIA only		Stage I and IIA, small tumors only	
	Unadjusted hazard ratio	95% confidence interval	Unadjusted hazard ratio	95% confidence interval	Unadjusted hazard ratio	95% confidence interval
KLF4 (type 1 *versus* type 2–4)	1.7	(0.94–3.22)	**2.8**	**(1.23–6.58)**	**4.3**	**(1.75–10.62)**
Lymph nodes positive *versus* negative	**3.2**	**(1.65–6.22)**	2.1	(0.81–5.37)	1.4	(0.50–3.70)
Stage[c]	**5.5**	**(2.88–10.64)**	0.7	(0.29–1.52)	1.2	(0.49–3.06)
Histological grade (high *versus* low)	**2.8**	**(1.53–5.24)**	1.9	(0.84–4.37)	**3.3**	**(1.32–8.28)**
Race (African American *versus* Caucasian)	**2.3**	**(1.29–4.12)**	2.0	(0.85–4.77)	**2.6**	**(1.03–6.45)**
Age (≤50 yrs *versus* >50 yrs)	1.3	(0.72–2.25)	1.1	(0.49–2.57)	1.4	(0.54–3.50)
BCL2 (> *versus* ≤ median immunoscore)	**0.4**	**(0.23–0.83)**	0.6	(0.24–1.34)	0.5	(0.19–1.18)
Ki67 (> *versus* ≤ median immunoscore)	1.3	(0.69–2.45)	0.9	(0.39–2.19)	1.5	(0.60–3.89)
p27KIP1 (> *versus* ≤ median immunoscore)	0.6	(0.31–1.12)	0.5	(0.20–1.16)	0.4	(0.15–1.00)
Estrogen receptor (positive *versus* negative)	0.8	(0.43–1.35)	1.4	(0.57–3.40)	0.7	(0.26–2.01)
Progesterone receptor (positive *versus* negative)	0.6	(0.32–1.07)	1.1	(0.47–2.43)	0.8	(0.31–1.89)

[a] Hazard ratios were considered to be statistically significant when the 95% confidence interval did not include 1.00. Statistically significant associations are highlighted in bold.

[b] The number of patients in each group is indicated in the corresponding panel of Fig. 2.

[c] For all tumors, the comparison was stage > I *versus* stage I. For stage I and IIA only, the comparison was stage IIA ($T_1N_1M_0$ and $T_2N_0M_0$) *versus* stage I. For stage I and IIA, small tumors only, the comparison was stage IIA ($T_1N_1M_0$) *versus* stage I.

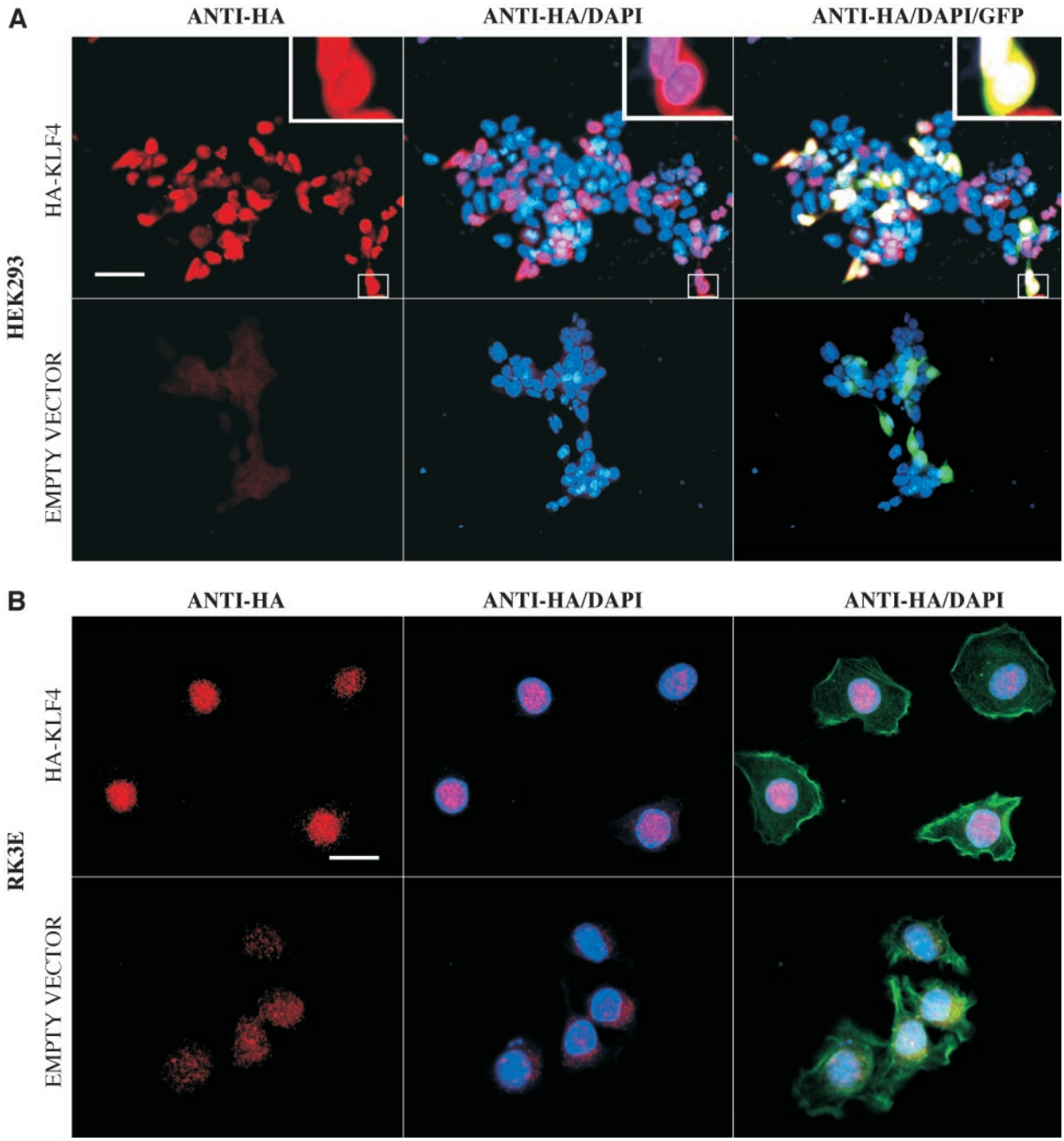

Fig. 5 Subcellular localization of epitope-tagged KLF4 *in vitro*. *A*, the human KLF4 cDNA was modified at the NH_2 terminus by addition of a hemagglutinin (HA) epitope. HEK293 cells were analyzed 48 h after transfection of HA-KLF4 (anti-HA, shown in *red*; *left panel*). Subcellular localization was determined by comparison to 4′,6-diamidino-2-phenylindole (DAPI)-stained nuclei (shown in *blue*; *middle panel*) and by expression of green fluorescent protein (GFP, shown in *green*; *right panel*). Colocalization of HA-KLF4 and DAPI results in a *pink color*. Cells transfected with empty vector were analyzed in parallel and served as a negative control (*bottom panels*). *B*, RK3E cells were transformed using an HA-KLF4 expression vector. HA-KLF4 cells (*top panel*) or vector control cells (*bottom panel*) were analyzed using anti-HA (shown in *red*; *left panel*). DAPI (shown in *blue*; *middle panel*) and phalloidin (shown in *green*; *right panel*) allowed visualization of the nucleus and cytoplasm, respectively. *Scale bar* for $A = 50$ μm; *scale bar* for $B = 20$ μm. *Insets* show the boxed areas at higher magnification.

outcome in this initial study, the high-risk group with T1-type 1 tumors included only 15 patients. In addition, the association between type 1 staining and outcome was not significant for all patients combined but only for the subset of patients with early-stage disease. Although KLF4 appeared to exhibit both sensitivity and specificity as a marker of poor outcome in these cases, a better appreciation of the hazard associated with type 1 staining will require analysis of larger groups of patients. Likewise, larger stud-

ies will reveal whether factors such as Ki67 expression, BCL2 expression, or stage at diagnosis may be associated with type 1 staining in small tumors.

Despite the limited study size, several lines of evidence support the association with clinical outcome. Importantly, our observation of poor outcome in T1-type 1 tumors resulted from testing of a hypothesis rather than from analysis of an arbitrary subset. We examined the potential association between outcome and type 1 staining because of the known role of KLF4 as a nuclear transcription factor and transforming oncogene. Patients with early-stage disease represent a subset in which prognostic markers may well exhibit a stronger association with outcome. For example, increased expression of BAG1, a regulator of cell proliferation and apoptosis, is associated with improved survival in patients with early-stage breast cancer (38). In that study, multivariate analysis revealed a stronger association in the node-negative subgroup ($P = 0.002$) than for the node-positive subgroup ($P > 0.050$) or for all stage I–II patients combined ($P = 0.008$). Keyomarsi *et al.* (35) reported the association between low molecular weight isoforms of cyclin E and death from breast cancer. In that study, the association was strongest in stage I and weakest in stage IV. In the current study, high histological grade was significantly associated with a poor outcome for both the small and large tumor subgroups, but the association was stronger for patients with small tumors. Furthermore, as knowledge of cancer biology and therapy improves, early-stage patients stand to benefit greatly from molecular staging. Thus, a careful analysis of this subgroup is justified.

In our study, type 1 staining was associated not only with death because of breast cancer, but also with high histological grade in the primary tumor, a well-recognized correlate of survival (39). The association with grade, as with the association with clinical outcome, was restricted to small tumors. As for clinical outcome and histological grade, the association between type 1 staining and reduced expression of BCL2 was stronger in small tumors.

The current study does not distinguish between active and passive roles for KLF4 in the aggressive phenotype of these early-stage tumors. Additional insight may come from analysis of KLF4-regulated genes (target genes). Increased expression of target genes in type 1 tumors *versus* type 4 tumors would be consistent with an active role because type 4 tumors likewise exhibit elevated nuclear expression of KLF4 but did not exhibit an aggressive phenotype. On the other hand, if preferential nuclear localization was a consequence of signaling through upstream regulators of KLF4, such signaling might promote the aggressive phenotype independently of KLF4 through parallel effector pathways. In this case, KLF4 would have only a passive role, and transcriptional targets might be similarly expressed in type 1 and type 4 tumors. We are currently using a conditional allele in combination with microarrays to identify target genes of KLF4.

Few markers associated with clinical outcome in breast cancer have been found to exhibit tumor size dependence. Although several possibilities may account for the nonassociation of type 1 staining and clinical outcome in large tumors, this result is particularly interesting given recent insights into KLF4 function as a transforming oncogene that induces a slow-growth phenotype (11). Potentially, the dual roles of KLF4 as both a transforming activity and an inhibitor of cell cycle progression could dissociate malignant potential from tumor size, leading to an aggressive or metastatic phenotype in tumors with a smaller diameter. Alternative explanations include the possibility that, in large tumors, the localization or transcriptional activity of KLF4 could be influenced by other signaling pathways or by the tumor microenvironment, thus confounding the associations observed in smaller tumors.

A complementary *in vitro* analysis revealed that KLF4 is virtually confined to the nucleus in the setting of malignant transformation of RK3E cells. This result supports the notion that KLF4 may function within the nucleus as a transcription factor to induce transformation. In addition to the nuclear expression observed *in vitro*, a prominent perinuclear component of KLF4 was detected following transient transfection. This preliminary observation warrants additional investigation because many transcription factors implicated in neoplasia exhibit regulated subcellular localization. The perinuclear staining we observed is consistent with similar regulation of KLF4, perhaps through tethering to a cytoplasmic protein. Interestingly, human KLF4 contains a putative SH3 domain binding site near the NH_2 terminus that could mediate such an interaction (40).

Although these results suggest that nuclear import and/or export of KLF4 may be regulated, upstream signaling pathways that mediate such regulation have not been identified. One interesting candidate is the TGF-β pathway. In vascular smooth muscle cells, TGF-β or other TGF-β-superfamily members induce the expression of smaller KLF4 isoforms and induce binding of KLF4 to TGF-β control elements found in the regulatory region of marker genes associated with smooth muscle differentiation (23, 41). The perinuclear localization of KLF4 that we observed *in vitro* provides a simple assay that may facilitate identification of such regulatory pathways. The possibility that this perinuclear staining is related to the more diffuse cytoplasmic staining observed in breast tumors also warrants further study.

The potential use of prognostic markers in the diagnosis and treatment of breast cancer has been reviewed (36, 42–44). A benefit of stratification of patients into distinct risk groups by molecular staging is that the use of known prognostic factors or the effectiveness of specific therapies may be enhanced in one of the subsets. For example, tumor size and stage at diagnosis could be enhanced as prognostic factors after identification and segregation of T1-type 1 cases, thus allowing for more effective selection of therapies and more efficient design of clinical trials. Although the current study associates KLF4 nuclear localization and clinical outcome in breast cancer, there is currently little evidence of a functional role for KLF4 in tumor progression. Currently, we are using short-term induction of KLF4 expression *in vitro* to identify transcriptional target genes and analyzing expression of these putative target genes within type 1 breast tumors and in a novel mouse model of KLF4-induced neoplasia. These studies may lead to a better understanding of signaling pathways that function upstream or downstream of KLF4 and may indicate whether KLF4 plays an important role in human tumor initiation or progression.

ACKNOWLEDGMENTS

We thank Cynthia Moore for assistance in immunostaining of tissue sections, Laura Gallitz for secretarial assistance, Glenda Williamson and Debra Martin for help with clinical data, and John Carpenter and Sam Beenken for critical reading of the manuscript.

REFERENCES

1. Hanahan D, Weinberg RA. The hallmarks of cancer. Cell 2000;100: 57–70.

2. Taipale J, Beachy PA. The Hedgehog and Wnt signaling pathways in cancer. Nature (Lond.) 2001;411:349–54.

3. Tetsu O, Mccormick F. β-Catenin regulates expression of cyclin D1 in colon carcinoma cells. Nature (Lond.) 1999;398:422–6.

4. He TC, Sparks AB, Rago C, et al. Identification of c-MYC as a target of the APC pathway. Science (Wash. DC) 1998;281:1509–12.

5. Kogerman P, Grimm T, Kogerman L, et al. Mammalian suppressor-of-fused modulates nuclear-cytoplasmic shuttling of Gli-1. Nat Cell Biol 1999;1:312–9.

6. Murone M, Luoh SM, Stone D, et al. Gli regulation by the opposing activities of fused and suppressor of fused. Nat Cell Biol 2000;2:310–2.

7. Taylor MD, Liu L, Raffel C, et al. Mutations in SUFU predispose to medulloblastoma. Nat Genet 2002;31:306–10.

8. Korinek V, Barker N, Morin PJ, et al. Constitutive transcriptional activation by a β-catenin-TCF complex in APC−/− colon carcinoma. Science (Wash. DC) 1997;275:1784–7.

9. Morin PJ, Sparks AB, Korinek V, et al. Activation of β-catenin-TCF signaling in colon cancer by mutations in β-catenin or APC. Science (Wash. DC) 1997;275:1787–90.

10. Kolligs FT, Kolligs B, Hajra KM, et al. γ-Catenin is regulated by the APC tumor suppressor and its oncogenic activity is distinct from that of β-catenin. Genes Dev 2000;14:1319–31.

11. Foster KW, Ren S, Louro ID, et al. Oncogene expression cloning by retroviral transduction of adenovirus E1a-immortalized rat kidney RK3E cells: transformation of a host with epithelial features by c-MYC and the zinc finger protein GKLF. Cell Growth Differ 1999;10:423–34.

12. Foster KW, Frost AR, McKie-Bell P, et al. Increase of GKLF messenger RNA and protein expression during progression of breast cancer. Cancer Res 2000;60:6488–95.

13. Segre JA, Bauer C, Fuchs E. Klf4 is a transcription factor required for establishing the barrier function of the skin. Nat Genet 1999;22:356–60.

14. Garrett-Sinha LA, Eberspaecher H, Seldin MF, de Crombrugghe B. A gene for a novel zinc-finger protein expressed in differentiated epithelial cells and transiently in certain mesenchymal cells. J Biol Chem 1996;271:31384–90.

15. Shields JM, Christy RJ, Yang VW. Identification and characterization of a gene encoding a gut-enriched Krüppel-like factor expressed during growth arrest. J Biol Chem 1996;271:20009–17.

16. Chen ZY, Shie JL, Tseng CC. Gut-enriched Kruppel-like factor represses ornithine decarboxylase gene expression and functions as checkpoint regulator in colonic cancer cells. J Biol Chem 2002;277:46831–9.

17. Shie JL, Chen ZY, Fu M, Pestell RG, Tseng CC. Gut-enriched Kruppel-like factor represses cyclin D1 promoter activity through Sp1 motif. Nucleic Acids Res 2000;28:2969–76.

18. Zhang W, Geiman DE, Shields JM, et al. The gut-enriched Kruppel-like factor (Kruppel-like factor 4) mediates the transactivating effect of p53 on the p21WAF1/Cip1 promoter. J Biol Chem 2000;275:18391–8.

19. Shields JM, Yang VW. Identification of the DNA sequence that interacts with the gut-enriched Krüppel-like factor. Nucleic Acids Res 1998;26:796–802.

20. Shields JM, Yang VW. Two potent nuclear localization signals in the gut-enriched Krüppel-like factor define a subfamily of closely related Krüppel proteins. J Biol Chem 1997;272:18504–7.

21. Pandya K, Townes TM. Basic residues within the Kruppel zinc finger DNA binding domains are the critical nuclear localization determinants of EKLF/KLF-1. J Biol Chem 2002;277:16304–12.

22. Quadrini KJ, Bieker JJ. Kruppel-like zinc fingers bind to nuclear import proteins and are required for efficient nuclear localization of erythroid Kruppel-like factor. J Biol Chem 2002;277:32243–52.

23. King KE, Iyemere VP, Weissberg PL, Shanahan CM. Kruppel-like factor 4 (KLF4/GKLF) is a target of bone morphogenetic proteins and transforming growth factor β1 in the regulation of vascular smooth muscle cell phenotype. J Biol Chem 2003;278:11661–9.

24. Greene FL, Page DL, Fleming ID, et al. (editors). Breast. In: AJCC cancer staging manual, New York: Springer-Verlag;2002. p. 223–40.

25. Frost AR, Sparks D, Grizzle WE. Methods of antigen recovery vary in their usefulness in unmasking specific antigens in immunohistochemistry. Appl Immunohistochem Mol Morphol 2000;8:236–43.

26. Grizzle WE, Myers RB, Manne U, Srivastava S. Immunohistochemical evaluation of biomarkers in prostatic and colorectal neoplasia. In: Hanausek M, Walaszek Z (editors). Methods in molecular medicine: tumor marker protocols. Totowa, NJ: Humana Press, Inc.;1998. p. 143–60.

27. Grizzle WE, Myers RB, Manne U, Stockard CR, Harkin LE, Srivastava S. Factors affecting immunohistochemical evaluation of biomarker expression in neoplasia. In: Hanausek M, Walaszek Z (editors). Methods in molecular medicine: tumor marker protocols. Totowa, NJ: Humana Press, Inc.;1998. p. 161–79.

28. Elston CW, Ellis IO. Pathological prognostic factors in breast cancer. I. The value of histological grade in breast cancer: experience from a large study with long-term follow-up. Histopathology 1991;19:403–10.

29. Fisher RA. The logic of inductive inference. J R Stat Soc [A] 1935;98:39–54.

30. Kaplan EL, Meier P. Nonparametric estimation from incomplete observations. J Am Stat Assoc 1958;53:457–81.

31. Cox DR. Regression models and life-tables. J R Stat Soc [B] 1972;34:187–220.

32. Jarvik JW, Telmer CA. Epitope tagging. Annu Rev Genet 1998;32: 601–18.

33. Ruppert JM, Vogelstein B, Kinzler KW. The zinc finger protein GLI transforms rodent cells in cooperation with adenovirus E1A. Mol Cell Biol 1991;11:1724–8.

34. Hutter RVP, Kennedy BJ, Murphy GP, O'Sullivan B, Sobin LH, Yarbro JW (editors). Breast. AJCC cancer staging manual, Philadelphia: Lippincott-Raven;1998. p. 171–80.

35. Keyomarsi K, Tucker SL, Buchholz TA, et al. Cyclin E and survival in patients with breast cancer. N. Engl J Med 2002;347:1566–75.

36. Clark GM. Prognostic and predictive factors. In: Harris JR, Lippman ME, Morrow M, Osborne CK (editors), Diseases of the breast. Philadelphia: Lippincott Williams & Wilkins;2000. p. 489–514.

37. Silvestrini R, Veneroni S, Daidone MG, et al. The Bcl-2 protein: a prognostic indicator strongly related to p53 protein in lymph node-negative breast cancer patients. J Natl Cancer Inst (Bethesda) 1994;86:499–504.

38. Turner BC, Krajewski S, Krajewska M, et al. BAG-1: a novel biomarker predicting long-term survival in early-stage breast cancer. J Clin Oncol 2001;19:992–1000.

39. Singletary SE, Allred C, Ashley P, et al. Staging system for breast cancer: revisions for the Ed. 6 of the AJCC cancer staging manual. Surg Clin N Am 2003;83:803–19.

40. Geiman DE, Han TT, Johnson JM, Yang VW. Transactivation and growth suppression by the gut-enriched Krüppel-like factor (Krüppel-like factor 4) are dependent on acidic amino acid residues and protein-protein interaction. Nucleic Acids Res 2000;28:1106–13.

41. Adam PJ, Regan CP, Hautmann MB, Owens GK. Positive- and negative-acting Kruppel-like transcription factors bind a transforming growth factor β control element required for expression of the smooth muscle cell differentiation marker SM22α *in vivo*. J Biol Chem 2000; 275:37798–806.

42. Beenken SW, Bland KI. Biomarkers for breast cancer. Minerva Chir 2002;57:437–48.

43. Morabito A, Magnani E, Gion M, et al. Prognostic and predictive indicators in operable breast cancer. Clin Breast Cancer 2003;3:381–90.

44. Klijn JGM, Berns EMJJ, Foekens JA. Prognostic and predictive factors and targets for therapy in breast cancer. In: Pasqualini JR (editor). Breast cancer: prognosis, treatment, and prevention. New York: Marcel Dekker, Inc.;2002. p. 93–124.

Clinical Cancer Research

Nuclear Localization of KLF4 Is Associated with an Aggressive Phenotype in Early-Stage Breast Cancer

Ashka Y. Pandya, Lynya I. Talley, Andra R. Frost, et al.

Clin Cancer Res 2004;10:2709-2719.